UC Santa Cruz
UC Santa Cruz Previously Published Works

Title

Calcium isotope composition of
Morozovella
over the late Paleoceneâearly Eocene

Permalink

Journal

ISSN

Authors

Kitch, Gabriella D
Jacobson, Andrew D
Harper, Dustin T
et al.

Publication Date

DOI

Peer reviewed

Calcium isotope composition of *Morozovella* over the late Paleocene–early Eocene

Gabriella D. Kitch[1], Andrew D. Jacobson[1], Dustin T. Harper[2], Matthew T. Hurtgen[1], Bradley B. Sageman[1] and James C. Zachos[3]

[1]Department of Earth and Planetary Sciences, Northwestern University, Evanston, Illinois 60208, USA
[2]Department of Geology, University of Kansas, Lawrence, Kansas 66045, USA
[3]Department of Earth and Planetary Sciences, University of California–Santa Cruz, Santa Cruz, California 95060, USA

ABSTRACT

Ocean acidification (OA) during the Paleocene-Eocene thermal maximum (PETM) likely caused a biocalcification crisis. The calcium isotope composition ($\delta^{44/40}$Ca) of primary carbonate producers may be sensitive to OA. To test this hypothesis, we constructed the first high-resolution, high-precision planktic foraminiferal $\delta^{44/40}$Ca records before and across the PETM. The records employed specimens of *Morozovella* spp. collected from Ocean Drilling Program Sites 1209 (Shatsky Rise, Pacific Ocean) and 1263 (Walvis Ridge, Atlantic Ocean). At Site 1209, $\delta^{44/40}$Ca values start at −1.33‰ during the Upper Paleocene and increase to a peak of −1.15‰ immediately before the negative carbon isotope excursion (CIE) that marks the PETM onset. Values remain elevated through the PETM interval and decrease into the earliest Eocene. A shorter-term record for Site 1263 shows a similar trend, although $\delta^{44/40}$Ca values are on average 0.22‰ lower and decrease shortly after the CIE onset. The trends support neither diagenetic overprinting, authigenic carbonate additions, nor changes in the $\delta^{44/40}$Ca value of seawater. Rather, they are consistent with a kinetic isotope effect, whereby calcite $\delta^{44/40}$Ca values inversely correlate with precipitation rate. Geologically rapid Ca isotope shifts appear to reflect the response of *Morozovella* to globally forced changes in the local carbonate geochemistry of seawater. All data combined suggest that the PETM-OA event occurred near the peak of a gradual reduction in seawater carbonate ion concentrations during a time of elevated atmospheric pCO$_2$, potentially driven by North Atlantic igneous province emplacement.

INTRODUCTION

Geologic records indicate widespread environmental disturbance during the Paleocene-Eocene thermal maximum (PETM) hyperthermal event (ca. 56 Ma). A negative carbon isotope excursion (CIE) of −2‰ to −3.5‰ in marine biogenic carbonates marks the PETM onset and signifies major carbon cycle disruption (Zachos et al., 2003, 2005). The abrupt and transient nature of the CIE points to forcing by CO$_2$ and other greenhouse gases (Zachos et al., 2003). Rapid injection of large amounts of CO$_2$ into the atmosphere causes transient decreases in ocean pH, carbonate ion concentrations ([CO$_3^{2-}$]), and carbonate mineral saturation states (Ω), collectively termed ocean acidification (OA) (Hönisch et al., 2012). Shoaling of the calcite compensation depth (Zachos et al., 2005) and decreased surface-ocean pH (Penman et al., 2014; Gut-

jahr et al., 2017) support OA during the PETM interval. The early Cenozoic ocean may have been particularly susceptible to OA given that equilibration with prevailing high-pCO$_2$ conditions reduced steady-state pH and [CO$_3^{2-}$] compared to other times with lower pCO$_2$ (Kump et al., 2009).

The calcium isotope ($\delta^{44/40}$Ca) system may trace OA-driven calcification stress. Laboratory experiments have demonstrated that the Ca isotope fractionation factor between inorganic calcite and water ($\Delta_{CaCO3–H2O} = \delta^{44/40}Ca_{CaCO3}$ − $\delta^{44/40}$Ca$_{H2O}$) varies as a function of precipitation rate, with slower rates yielding higher $\delta^{44/40}$Ca values and vice versa for faster rates (e.g., Tang et al., 2008). Moreover, recent evidence shows that some natural biogenic carbonates work similarly (Wang et al., 2021). Calcium isotope records generated across other proposed OA

events, such as oceanic anoxic events 1a and 2 (Du Vivier et al., 2015; Wang et al., 2021) and the end-Cretaceous (Linzmeier et al., 2020), show positive excursions consistent with reductions in $\Delta_{CaCO3 – H2O}$ due to volcanic CO$_2$ emissions. Bulk sediments spanning the PETM also show positive $\delta^{44/40}$Ca excursions, but these likely reflect authigenic carbonate formation (Griffith et al., 2015). Noting that lower pH and [CO$_3^{2-}$] typically cause foraminifera to reduce their calcification rates (Osborne et al., 2016; Davis et al. 2017), and that foraminiferal tests provide a more accurate archive of seawater geochemistry than the average signal from bulk sediments (Sime et al., 2007), we generated the first foraminiferal $\delta^{44/40}$Ca records spanning the PETM to test for OA signals.

MATERIALS AND METHODS

Calcium isotope ratios (^{44}Ca/^{40}Ca) were measured at Northwestern University (Illinois, USA) using a high-precision ^{43}Ca-^{42}Ca double-spike thermal ionization mass spectrometry (TIMS) method. We analyzed specimens of planktic foraminifera *Morozovella* spp. collected from Ocean Drilling Program (ODP) Sites 1209 (Shatsky Rise, Pacific Ocean) and 1263 (Walvis Ridge, Atlantic Ocean; Fig. 1). We focused on *Morozovella* based on evidence that this taxon occupied the photic zone and robustly captured B isotope (δ^{11}B) signals of surface-water acidification (Penman et al., 2014). Different species were employed due to low sample availability. However, all *Morozovella* spp. dwelled at a similarly shallow depths (Birch et al., 2012), and no differences were observed for replicate/duplicate measurements, consistent with previous assertions that different foraminiferal species of the same genus display limited Ca isotope variability (Sime et al., 2007). Each sample
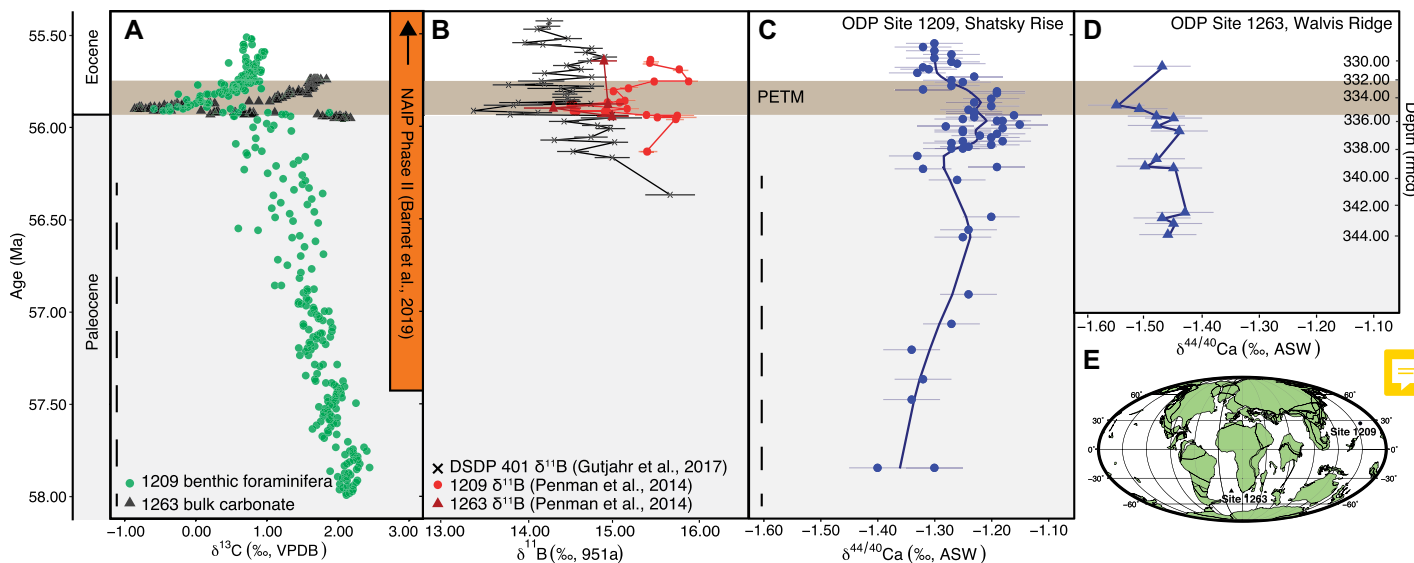
Figure 1. (A) Ocean Drilling Project (ODP) Leg 198, Site 1209 (Shatsky Rise, Pacific Ocean), $\delta^{13}C$ values from the benthic foraminifera *Nuttalides truempyi* (Westerhold et al., 2018) and ODP Leg 208, Site 1263 (Walvis Ridge, Atlantic Ocean), bulk carbonate $\delta^{13}C$ values (Zachos et al., 2005) plotted against age (Westerhold et al., 2017, 2018). North Atlantic igneous province (NAIP) volcanism is plotted for reference (Barnet et al., 2019). VPDB—Vienna Peedee belemnite. (B) Foraminiferal $\delta^{11}B$ values for ODP Sites 1209 and 1263 (Penman et al., 2014), as well as Deep Sea Drilling Project (DSDP) Site 408 (Meriadzek Terrace on the north Biscay margin; Gutjahr et al., 2017). (C,D) $\delta^{44/40}Ca$ records from planktic foraminifera *Morozovella* spp. (C) ODP Site 1209 and (D) ODP Site 1263 plotted against age (Westerhold et al., 2017) and depth. Curves represent locally weighted smoothing (LOESS) span of 35. Error bars for C and D represent $2\sigma_{SD} = \pm 0.05‰$. Dashed lines in A and C indicate correlation time series. PETM—Paleocene-Eocene thermal maximum; rmcd—revised meters composite depth. (E) Map showing continental configuration for 54.0 Ma demonstrates paleolatitudes of ~27°N for ODP Site 1209 and ~42°S for Site 1263 (van Hinsbergen et al., 2015).

consisted of five individual foraminifera. In total, we analyzed 73 samples. An additional 37 samples were measured to test cleaning procedures, which revealed negligible effects. Data are reported in delta notation relative to Ocean Scientific International Ltd. (OSIL) Atlantic seawater (ASW). Repeated analyses of standards and samples yielded a reproducibility of $\pm 0.05‰$ ($2\sigma_{SD}$). See the Supplemental Material[1] for more information.

RESULTS
ODP Site 1209

The average $\delta^{44/40}Ca$ value at ODP Site 1209 equals $-1.27‰ \pm 0.05‰$ ($2\sigma_{SD}$, $n = 59$). Values begin at $-1.33‰$ (57.80 Ma) and steadily increase by ~0.10‰ until ca. 56.20 Ma. At ca. 56.20 Ma, values briefly decrease, then increase again by ~0.13‰ ~170 k.y. prior to the CIE body, and remain elevated through the CIE body before decreasing by ~0.13‰ during the CIE recovery (Figs. 1 and 2). Increasing $\delta^{44/40}Ca$ values leading up to the PETM correspond with decreasing $\delta^{13}C$ values ($p < 0.001$; Fig. 3). High $\delta^{44/40}Ca$ values occur in the same interval where low $\delta^{11}B$ and B/Ca values indicate OA, and the subsequent decrease occurs where $\delta^{11}B$

and B/Ca indicate recovery from OA (Fig. 2; Penman et al., 2014; Westerhold et al., 2018).

ODP Site 1263

At $-1.49‰ \pm 0.05‰$ ($2\sigma_{SD}$, $n = 14$; Fig. 2), the average $\delta^{44/40}Ca$ value at ODP Site 1263 is 0.22‰ lower compared to Site 1209. Values ranging between $-1.55‰$ and $-1.45‰$ generally define the same secular trend as Site 1209, including a maximum prior to the CIE body. Values decrease through the PETM interval (Figs. 1 and 4), but as with Site 1209, the $\delta^{44/40}Ca$ and $\delta^{11}B$ recoveries coincide.

DISCUSSION
Diagenesis and Authigenesis

Foraminiferal tests from both sites reveal recrystallization in the form of "frost," consistent with diagenetic mineral replacement (Fantle et al., 2020). However, statistical analyses of $\delta^{44/40}Ca$ against sedimentological data, such as fragmentation indices and sedimentation rates (see the Supplemental Material), do not support replacement under fluid-buffered conditions at the sediment-water interface. Furthermore, diagenetic mineral replacement may affect other proxies, such as $\delta^{11}B$ and B/Ca (Fantle et al., 2020), but these measurements applied to ODP Sites 1209 and 1263 revealed no evidence for alteration (Penman et al., 2014). These results support expectations that carbonate-rich pelagic sediments recrystallize under rock-buffered conditions, which preserve primary geochemical signals (Higgins et al., 2018). Numerical models

predict that OA-driven authigenic carbonate additions can elevate bulk carbonate $\delta^{44/40}Ca$ values, especially during "alkalinity overshoots" that occur in the aftermath of OA events (Fantle and Ridgwell, 2020). However, the peak $\delta^{44/40}Ca$ values reported here occur before the PETM CIE onset. These observations indicate that microfossil $\delta^{44/40}Ca$ records are resistant to authigenic signals that may otherwise affect bulk carbonate records.

Kinetic Effects

Calcium isotope fluctuations before and across the CIE body occur rapidly relative to the long oceanic residence time of Ca ($\tau_{Ca} = $ ~1 m.y.). Input-output flux perturbations that drive changes in the $\delta^{44/40}Ca$ value of seawater cannot explain such patterns (Komar and Zeebe, 2011). The PETM was a time of profound warming (Zachos et al., 2003), and foraminiferal culturing studies point to the temperature dependence of $\Delta_{CaCO3 - H2O}$ (Gussone et al., 2003). However, the temperature sensitivity is low (Sime et al., 2005), and $\delta^{44/40}Ca$ values at ODP Site 1209 show no relationship to established temperature-sensitive proxies, such as Mg/Ca ratios (see the Supplemental Material; Penman et al., 2014; Zachos et al., 2003).

Negative $\delta^{11}B$ excursions at Sites 1209 and 1263, and negative B/Ca excursions at Site 1209 indicate reduced pH and elevated dissolved inorganic carbon (DIC) during the event (Penman et al., 2014), which raises the
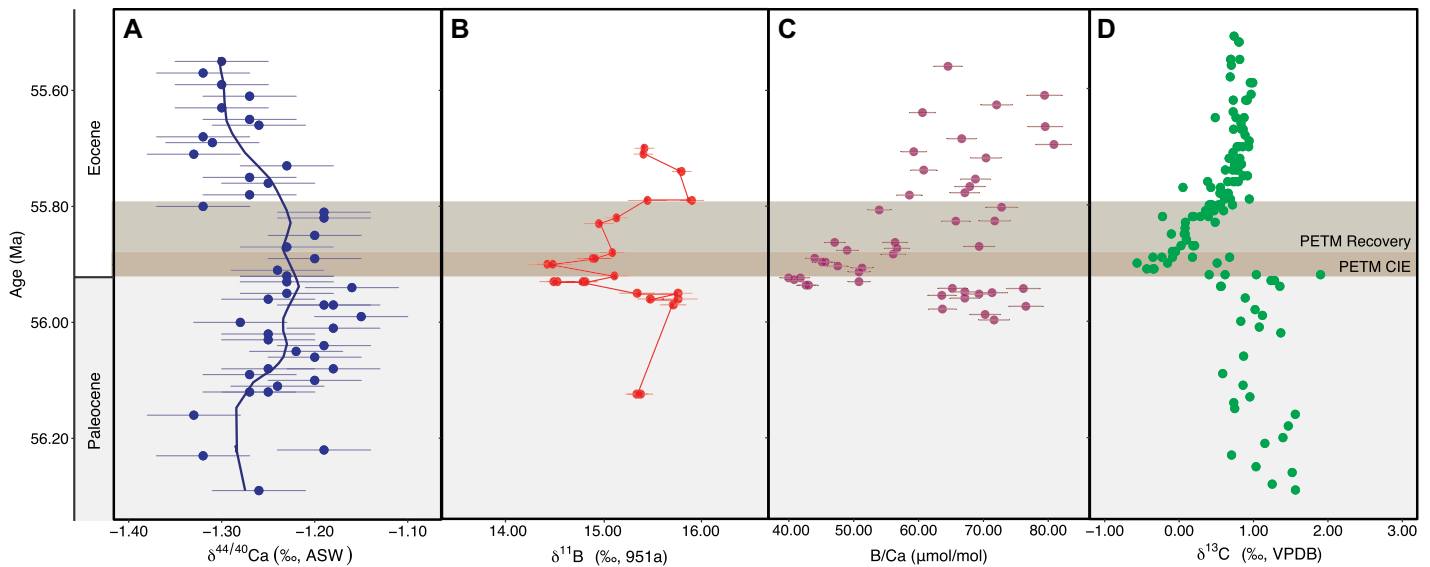
Figure 2. (A) Ocean Drilling Project (ODP) Site 1209 (Shatsky Rise, Pacific Ocean) $\delta^{44/40}$Ca records from planktic foraminifera *Morozovella* spp. (this study), (B) *Morozovella velascoensis* δ^{11}B (Penman et al., 2014), (C) *M. velascoensis* B/Ca (Penman et al., 2014), and (D) *Nuttalides truempyi* δ^{13}C values plotted against age (Westerhold et al., 2018). See the Supplemental Material (see footnote 1) for more discussion concerning $\delta^{44/40}$Ca and δ^{11}B. Error bars represent $2\sigma_{SD}$ for $\delta^{44/40}$Ca (±0.05‰) and B/Ca and 2 standard error mean for δ^{11}B. ASW—OSIL Atlantic seawater; VPDB—Vienna Peedee belemnite; PETM—Paleocene-Eocene thermal maximum; CIE—carbon isotope excursion.

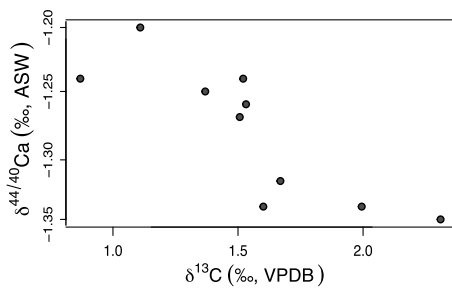**Figure 3.** $\delta^{44/40}$Ca records from planktic foraminifera *Morozovella* spp. (this study) and δ^{13}C from benthic foraminifera *Nuttalides truempyi* (Westerhold et al., 2018) from Ocean Drilling Project (ODP) Site 1209 (Shatsky Rise, Pacific Ocean) show significant negative correlation ($p <0.01$, $n = 10$, $R^2 = -0.77$). ASW—OSIL Atlantic seawater; VPDB—Vienna Peedee belemnite.

possibility that *Morozovella* calcification rates decreased. It is widely accepted that rate-dependent mechanisms govern Ca isotope fractionation during inorganic carbonate mineral precipitation (Tang et al., 2008; DePaolo, 2011). As precipitation rates increase, the system approaches a kinetic limit, whereby the magnitude of $\Delta_{CaCO3 - H2O}$ increases. Conversely, as precipitation rates decrease, the system approaches an equilibrium limit, causing the magnitude of $\Delta_{CaCO3 - H2O}$ to decrease. Foraminifera decrease calcification under lower $[CO_3^{2-}]$ (Osborne et al., 2016; Davis et al., 2017), and foraminiferal Ca isotope fractionation may resemble that for inorganic calcite (Gussone et al., 2003). However, no foraminiferal culturing studies have quantified Ca isotope effects under conditions that simulate

OA. One experiment that used growth rates to constrain precipitation rates observed a decrease in the magnitude of $\Delta_{CaCO3 - H2O}$ at higher $[CO_3^{2-}]$ (Kısakürek et al., 2011). The apparent discrepancy with inorganic experiments could reflect that $[CO_3^{2-}]$ was manipulated by changing alkalinity and pH rather than DIC. In addition, growth rates were determined by changes in shell mass, but without normalizing to shell size (Osborne et al., 2016), it is not possible to discriminate whether $[CO_3^{2-}]$ or temperature controls shell growth (de Villiers et al., 2004). A coccolithophorid culturing experiment that more closely simulated the effects of OA observed the anticipated correspondence among pCO$_2$, calcification rates, and $\Delta_{CaCO3 - H2O}$ (Mejía et al., 2018), although we note that foraminifera and coccolithophores calcify in fundamentally different ways (Erez, 2003).

While more culturing studies are needed to quantitatively interpret biogenic $\delta^{44/40}$Ca records, the apparent relationship between $\delta^{44/40}$Ca and established OA proxies observed here supports qualitative interpretation of aqueous carbonate system control. At Site 1209, the protracted negative δ^{11}B excursion during the CIE body corresponds to a similarly protracted positive $\delta^{44/40}$Ca excursion that began prior to, and persisted through, the event. At Site 1263, the brief negative δ^{11}B excursion during the CIE body corresponds to a brief positive $\delta^{44/40}$Ca excursion, which, similar to Site 1209, began prior to the event. Potential truncation at Site 1209 at the PETM onset (Haynes and Hönisch, 2020) may explain the lower than hypothesized inverse correlation between $\delta^{44/40}$Ca and δ^{11}B (see the Supplemental Material). Nonetheless, coupling

between the proxies is particularly evident in the recovery phase. Positive $\delta^{44/40}$Ca excursions measured for oceanic anoxic event 1a (OAE1a; Wang et al., 2021) and the end-Cretaceous (Linzmeier et al., 2020) also began prior to their associated CIEs. Furthermore, multiproxy comparisons applied to the OAE1a bulk carbonates reveals precipitation rate–dependent control of $\Delta_{CaCO3 - H2O}$ (Wang et al., 2021), and the end-Cretaceous record correlates with sedimentological indicators of saturation state in a way consistent with aqueous carbonate system control (Linzmeier et al., 2020).

Our interpretation predicts that gradual acidification may have preceded the PETM interval (Fig. 2). While both sites lack sufficient pre-CIE δ^{11}B data to directly corroborate this hypothesis, a longer-term record from Deep Sea Drilling Project Site 408 in the North Atlantic provides support (Fig. 1; Gutjahr et al., 2017). Here, δ^{11}B values, and pH by extension, were higher before the CIE and declined into the interval. The decreased biocalcification implied by $\delta^{44/40}$Ca may indicate concomitant reductions in $[CO_3^{2-}]$. Finally, the longer-term $\delta^{44/40}$Ca record at ODP Site 1209 inversely correlates with the δ^{13}C record (Fig. 3). Decreasing δ^{13}C values toward the PETM CIE are consistent with CO$_2$ inputs from emplacement of the North American igneous province (Barnet et al., 2019), which we suggest drove changes in Ca isotope fractionation. The inferred control of increasing pCO$_2$ on Ca isotope variability further implies that biological compensation may have increased surface-water alkalinity (Boudreau et al., 2018) and elevated the buffering capacity of the oceans (Haynes and Hönisch, 2020).
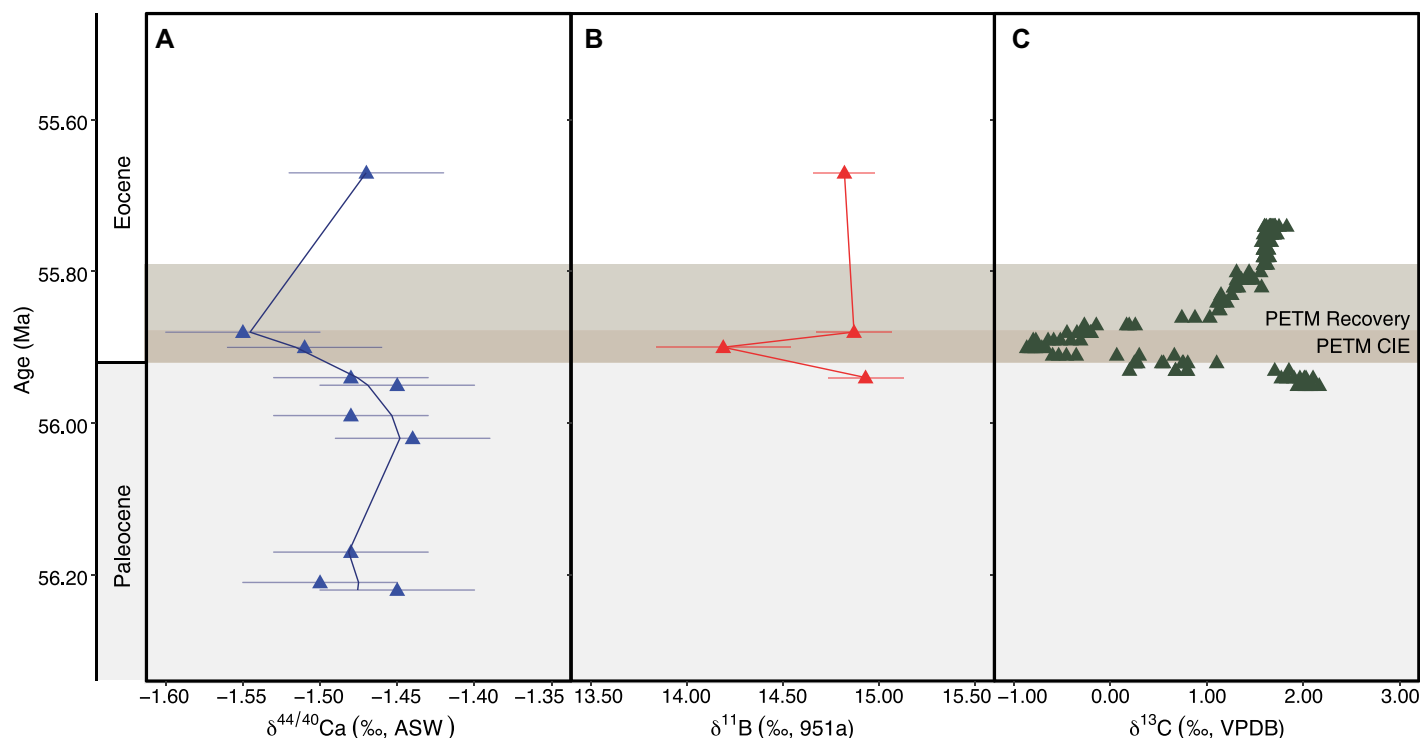
Figure 4. (A) Ocean Drilling Project (ODP) Site 1263 (Walvis Ridge, Atlantic Ocean) $\delta^{44/40}Ca$ records from planktic foraminifera *Morozovella* spp. (this study), (B) $\delta^{11}B$ (Penman et al., 2014), and (C) bulk carbonate $\delta^{13}C$ values (Zachos et al., 2005) plotted against age (Westerhold et al., 2017). Error bars represent $2\sigma_{SD}$ for $\delta^{44/40}Ca$ (±0.05‰) and 2 standard error of mean for $\delta^{11}B$. ASW—OSIL Atlantic seawater; VPDB—Vienna Peedee belemnite; PETM—Paleocene-Eocene thermal maximum; CIE—carbon isotope excursion.

Global Forcing with Local Expression

High-precision measurements clearly resolve an absolute delta value offset between ODP Sites 1209 and 1263. Given the long residence time of Ca in seawater, it is improbable that the Pacific and Atlantic Oceans sustained unique $\delta^{44/40}Ca$ values. Rather, our interpretation above implies that *Morozovella* individuals at Site 1209 experienced net lower precipitation rates compared to those at Site 1263. This suggests that surface waters at Site 1209 had lower [CO_3^{2-}] and pH compared to Site 1263, although model simulations suggest that the Atlantic Ocean may have been overall more corrosive during the PETM (Zeebe and Zachos, 2007). Without a mechanistic understanding of how foraminiferal $\delta^{44/40}Ca$ values respond to OA-driven calcification stress, we can only hypothesize that the absolute offset reflects an organismal response to locally heterogenous [CO_3^{2-}]. Relatively greater upwelling at Site 1263, as observed during later hyperthermals (Harper et al., 2019), may have increased organic productivity and export (Ma et al., 2014), thereby yielding higher surface-water [CO_3^{2-}]. Moreover, shoaling of the carbonate compensation depth at Site 1263 (Zachos et al., 2005) could have sped up carbonate system recovery by increasing surface-water [CO_3^{2-}] during the PETM, as recorded by the relatively short-lived $\delta^{11}B$ and $\delta^{44/40}Ca$ excursions.

CONCLUSION

Foraminiferal Ca isotope records generated from ODP Sites 1209 (Pacific) and 1263 (Atlantic) have different $\delta^{44/40}Ca$ values that define complementary secular trends before and across the PETM CIE. Interpreted in context with established carbonate system proxies, such as $\delta^{11}B$ and B/Ca, the data point to kinetic control of $\Delta_{CaCO3 - H2O}$. At Site 1209, a gradual rise in $\delta^{44/40}Ca$ values ~1.5 m.y. before the PETM corresponds to a similarly gradual decline in $\delta^{13}C$ values. Both sites show elevated $\delta^{44/40}Ca$ values preceding the CIE onset. We hypothesize that increasing pCO_2 levels, likely from North Atlantic igneous province emplacement, reduced [CO_3^{2-}], *Morozovella* calcification rates, and, thus, $\Delta_{CaCO3 - H2O}$. While more research is needed to better understand how foraminiferal Ca isotope fractionation responds to OA, our findings suggest that *Morozovella* calcification stress began prior to the PETM interval. To the extent that *Morozovella* typifies other planktic foraminifera, our results imply that reduced foraminiferal calcification prior to and during the PETM helped to dampen OA and contributed to elevated surface-ocean alkalinity during and after the event.

REFERENCES CITED
Barnet, J.S., Littler, K., Westerhold, T., Kroon, D., Leng, M.J., Bailey, I., Röhl, U., and Zachos, J.C., 2019, A high-fidelity benthic stable isotope record of Late Cretaceous–early Eocene climate change and carbon-cycling: Paleoceanography and Paleoclimatology, v. 34, p. 672–691, https://doi.org/10.1029/2019PA003556.
Birch, H.S., Coxall, H.K., and Pearson, P.N., 2012, Evolutionary ecology of early Paleocene planktonic foraminifera: Size, depth habitat and symbiosis: Paleobiology, v. 38, p. 374–390, https://doi.org/10.1666/11027.1.
Boudreau, B.P., Middelburg, J.J., and Luo, Y., 2018, The role of calcification in carbonate compensation: Nature Geoscience, v. 11, p. 894–900, https://doi.org/10.1038/s41561-018-0259-5.
Davis, C.V., Fehrenbacher, J.S., Hill, T.M., Russell, A.D., and Spero, H.J., 2017, Relationships between temperature, pH, and crusting on Mg/Ca ratios in laboratory-grown *Neogloboquadrina* foraminifera: Paleoceanography, v. 32, p. 1137–1152, https://doi.org/10.1002/2017PA003111.
DePaolo, D.J., 2011, Surface kinetic model for isotopic and trace element fractionation during

precipitation of calcite from aqueous solutions: Geochimica et Cosmochimica Acta, v. 75, p. 1039–1056, https://doi.org/10.1016/j.gca.2010.11.020.

De Villiers, S., 2004, Optimum growth conditions as opposed to calcite saturation as a control on the calcification rate and shell-weight of marine foraminifera: Marine Biology, v. 144, p. 45–49, https://doi.org/10.1007/s00227-003-1183-8.

Du Vivier, A.D.C., Jacobson, A.D., Lehn, G.O., Selby, D., Hurtgen, M.T., and Sageman, B.B., 2015, Ca isotope stratigraphy across the Cenomanian–Turonian OAE 2: Links between volcanism, seawater geochemistry, and the carbonate fractionation factor: Earth and Planetary Science Letters, v. 416, p. 121–131, https://doi.org/10.1016/j.epsl.2015.02.001.

Erez, J., 2003, The source of ions for biomineralization in foraminifera and their implications for paleoceanographic proxies: Reviews in Mineralogy and Geochemistry, v. 54, p. 115–149, https://doi.org/10.2113/0540115.

Fantle, M.S., and Ridgwell, A., 2020, Towards an understanding of the Ca isotopic signal related to ocean acidification and alkalinity overshoots in the rock record: Chemical Geology, v. 547, 119672, https://doi.org/10.1016/j.chemgeo.2020.119672.

Fantle, M.S., Barnes, B.D., and Lau, K.V., 2020, The role of diagenesis in shaping the geochemistry of the marine carbonate record: Annual Review of Earth and Planetary Sciences, v. 48, p. 549–583, https://doi.org/10.1146/annurev-earth-073019-060021.

Griffith, E.M., Fantle, M.S., Eisenhauer, A., Paytan, A., and Bullen, T.D., 2015, Effects of ocean acidification on the marine calcium isotope record at the Paleocene-Eocene thermal maximum: Earth and Planetary Science Letters, v. 419, p. 81–92, https://doi.org/10.1016/j.epsl.2015.03.010.

Gussone, N., Eisenhauer, A., Heuser, A., Dietzel, M., Bock, B., Böhm, F., Spero, H.J., Lea, D.W., Bijma, J., and Nägler, T.F., 2003, Model for kinetic effects on calcium isotope fractionation (δ^{44}Ca) in inorganic aragonite and cultured planktonic foraminifera: Geochimica et Cosmochimica Acta, v. 67, p. 1375–1382, https://doi.org/10.1016/S0016-7037(02)01296-6.

Gutjahr, M., Ridgwell, A., Sexton, P.F., Anagnostou, E., Pearson, P.N., Pälike, H., Norris, R.D., Thomas, E., and Foster, G.L., 2017, Very large release of mostly volcanic carbon during the Palaeocene-Eocene thermal maximum: Nature, v. 548, p. 573, https://doi.org/10.1038/nature23646.

Harper, D., Hönisch, B., Zeebe, R., Shaffer, G., Haynes, L., Thomas, E., and Zachos, J., 2019, The magnitude of surface ocean acidification and carbon release during Eocene thermal maximum 2 (ETM-2) and the Paleocene-Eocene thermal maximum (PETM): Paleoceanography and Paleoclimatology, v. 35, e2019PA003699, https://doi.org/10.1029/2019PA003699.

Haynes, L.L., and Hönisch, B., 2020, The seawater carbon inventory at the Paleocene–Eocene

Thermal Maximum: Proceedings of the National Academy of Sciences of the United States of America, v. 117, p. 24088–24095. https://doi.org/10.1073/pnas.2003197117.

Higgins, J., Blättler, C., Lundstrom, E., Santiago-Ramos, D., Akhtar, A., Ahm, A.C., Bialik, O., Holmden, C., Bradbury, H., and Murray, S., 2018, Mineralogy, early marine diagenesis, and the chemistry of shallow-water carbonate sediments: Geochimica et Cosmochimica Acta, v. 220, p. 512–534, https://doi.org/10.1016/j.gca.2017.09.046.

Hönisch, B., et al., 2012, The geological record of ocean acidification: Science, v. 335, p. 1058–1063, https://doi.org/10.1126/science.1208277.

Kısakürek, B., Eisenhauer, A., Böhm, F., Hathorne, E.C., and Erez, J., 2011, Controls on calcium isotope fractionation in cultured planktic foraminifera, *Globigerinoides ruber* and *Globigerinella siphonifera*: Geochimica et Cosmochimica Acta, v. 75, p. 427–443, https://doi.org/10.1016/j.gca.2010.10.015.

Komar, N., and Zeebe, R., 2011, Oceanic calcium changes from enhanced weathering during the Paleocene-Eocene thermal maximum: No effect on calcium-based proxies: Paleoceanography, v. 26, PA3211, https://doi.org/10.1029/2010PA001979.

Kump, L.R., Bralower, T.J., and Ridgwell, A., 2009, Ocean acidification in deep time: Oceanography (Washington, D.C.), v. 22, no. 4, p. 94–107, https://doi.org/10.5670/oceanog.2009.100.

Linzmeier, B.J., Jacobson, A.D., Sageman, B.B., Hurtgen, M.T., Ankney, M.E., Petersen, S.V., Tobin, T.S., Kitch, G.D., and Wang, J., 2020, Calcium isotope evidence for environmental variability before and across the Cretaceous-Paleogene mass extinction: Geology, v. 48, p. 34–38, https://doi.org/10.1130/G46431.1.

Ma, Z., Gray, E., Thomas, E., Murphy, B., Zachos, J., and Paytan, A., 2014, Carbon sequestration during the Paleocene-Eocene thermal maximum by an efficient biological pump: Nature Geoscience, v. 7, p. 382–388, https://doi.org/10.1038/ngeo2139.

Mejía, L.M., Paytan, A., Eisenhauer, A., Böhm, F., Kolevica, A., Bolton, C., Méndez-Vicente, A., Abrevaya, L., Isensee, K., and Stoll, H., 2018, Controls over $\delta^{44/40}$Ca and Sr/Ca variations in coccoliths: New perspectives from laboratory cultures and cellular models: Earth and Planetary Science Letters, v. 481, p. 48–60, https://doi.org/10.1016/j.epsl.2017.10.013.

Osborne, E.B., Thunell, R.C., Marshall, B.J., Holm, J.A., Tappa, E.J., Benitez-Nelson, C., Cai, W.-J., and Chen, B., 2016, Calcification of the planktonic foraminifera *Globigerina bulloides* and carbonate ion concentration: Results from the Santa Barbara Basin: Paleoceanography, v. 31, p. 1083–1102, https://doi.org/10.1002/2016PA002933.

Penman, D.E., Hönisch, B., Zeebe, R.E., Thomas, E., and Zachos, J.C., 2014, Rapid and sustained surface ocean acidification during the Paleocene-Eocene thermal maximum: Pale-

oceanography, v. 29, p. 357–369, https://doi.org/10.1002/2014PA002621.

Sime, N.G., Christina, L., and Galy, A., 2005, Negligible temperature dependence of calcium isotope fractionation in 12 species of planktonic foraminifera: Earth and Planetary Science Letters, v. 232, p. 51–66, https://doi.org/10.1016/j.epsl.2005.01.011.

Sime, N.G., De La Rocha, C.L., Tipper, E.T., Tripati, A., Galy, A., and Bickle, M.J., 2007, Interpreting the Ca isotope record of marine biogenic carbonates: Geochimica et Cosmochimica Acta, v. 71, p. 3979–3989, https://doi.org/10.1016/j.gca.2007.06.009.

Tang, J., Dietzel, M., Böhm, F., Köhler, S.J., and Eisenhauer, A., 2008, Sr²⁺/Ca²⁺ and ⁴⁴Ca/⁴⁰Ca fractionation during inorganic calcite formation: II. Ca isotopes: Geochimica et Cosmochimica Acta, v. 72, p. 3733–3745, https://doi.org/10.1016/j.gca.2008.05.033.

van Hinsbergen, D.J.J., De Groot, L.V., Van Schaik, S.J., Spakman, W., Bijl, P.K., Sluijs, A., Langereis, C.G., and Brinkhuis, H., 2015, A paleolatitude calculator for paleoclimate studies: PLoS One, v. 10, p. e0126946, https://doi.org/10.1371/journal.pone.0126946.

Wang, J., Jacobson, A.D., Sageman, B.B., and Hurtgen, M.T., 2021, Stable Ca and Sr isotopes support volcanically triggered biocalcification crisis during oceanic anoxic event 1a: Geology, https://doi.org/10.1130/G47945.1 (in press).

Westerhold, T., Röhl, U., Frederichs, T., Agnini, C., Raffi, I., Zachos, J.C., and Wilkens, R.H., 2017, Astronomical calibration of the Ypresian timescale: Implications for seafloor spreading rates and the chaotic behavior of the solar system?: Climate of the Past, v. 13, p. 1129–1152, https://doi.org/10.5194/cp-13-1129-2017.

Westerhold, T., Röhl, U., Donner, B., and Zachos, J., 2018, Global extent of early Eocene hyperthermal events—A new Pacific benthic foraminiferal isotope record from Shatsky Rise (ODP Site 1209): Paleoceanography and Paleoclimatology, v. 33, p. 626–642, https://doi.org/10.1029/2017PA003306.

Zachos, J.C., Wara, M.W., Bohaty, S., Delaney, M.L., Petrizzo, M.R., Brill, A., Bralower, T.J., and Premoli-Silva, I., 2003, A transient rise in tropical sea surface temperature during the Paleocene-Eocene thermal maximum: Science, v. 302, p. 1551–1554, https://doi.org/10.1126/science.1090110.

Zachos, J.C., Röhl, U., Schellenberg, S.A., Sluijs, A., Hodell, D.A., Kelly, D.C., Thomas, E., Nicolo, M., Raffi, I., and Lourens, L.J., 2005, Rapid acidification of the ocean during the Paleocene-Eocene thermal maximum: Science, v. 308, p. 1611–1615, https://doi.org/10.1126/science.1109004.

Zeebe, R.E., and Zachos, J.C., 2007, Reversed deep-sea carbonate ion basin gradient during Paleocene-Eocene thermal maximum: Paleoceanography and Paleoclimatology, v. 22, PA3201, https://doi.org/10.1029/2006PA001395.